J. Biochem. 120, 1104-1110 (1996)

Effects of Subtilisin Cleavage of Monomeric Actin on Its Nucleotide Binding

Atsushi Ooi*,[1] and Koshin Mihashi[†]

[†]*Faculty of Bioresources, Mie University, Kamihama 1515, Tsu, 514; and* [†]*Graduate School of Polymathematics, Nagoya University, Furo-cho, Chikusa-ku, Nagoya 464-01*

Received for publication, June 24, 1996

The kinetics of ATP exchange on subtilisin-cleaved G-actin was investigated by measuring the fluorescence of 1,N^6-ethenoadenosine 5′-triphosphate. The apparent dissociation rate of ATP (k_{-ATP}) was 2.8-fold larger than that of intact G-actin in the presence of 300 μM free Ca^{2+}. Analysis of the dependence of k_{-ATP} on free Ca^{2+} showed that the dissociation rate constant of tightly bound Ca^{2+} was not significantly changed by subtilisin cleavage. On the other hand, an equilibrium binding study using 8-amino-2-[(2-amino-5-methylphenoxy)-methyl]-6-methoxyquinoline *N,N,N′,N′*-tetraacetic acid (Quin 2) showed that the affinity of tightly bound Ca^{2+} for G-actin was reduced by about 13-fold after subtilisin treatment. Consequently, the stabilization by Ca^{2+} of ATP was weak in cleaved G-actin. Furthermore, the kinetic analysis of ATP exchange revealed that the binding equilibrium between ATP and divalent cation-free cleaved G-actin was much slower than that in the case of intact G-actin.

Key words: actin, divalent cation, nucleotide, subtilisin, surface loop.

G-Actin has one tightly bound nucleotide, which is exchangeable with exogenous nucleotide in solution. The nucleotide exchangeability of G-actin plays an important role in the monomer-polymer transition cycle of actin (*1*). It is well established that nucleotide exchange of actin is strongly influenced by the presence of divalent cation in solution (*2, 3*). Recently, biochemical studies indicated that divalent cations interact directly with the bound nucleotide on actin and stabilize it (*4, 5*).

The three-dimensional structure of actin-DNaseI complex determined by Kabsch *et al.* has revealed that both nucleotide and divalent cation are located on the central cleft between the small and the large domains of actin (*6*). There is much evidence concerning intramolecular communication between the cleft region and other structural elements of G-actin. For example, the C-terminal region around the Cys374 residue is sensitive to bound nucleotide and/or divalent cation (*7, 8*). The reverse communication from the C-terminal segment to the cleft was indicated by a change of the nucleotide exchange rate in actin chemically modified at Cys374 (*9*) and in truncated actin devoid of the last three C-terminal residues (*10*). Based on a proteolytic study, Strzelecka-Golaszewska *et al.* reported that a conformational change due to the substitution of bound divalent cation and/or bound nucleotide was also observed in subdomain 2 (*11*). Very recently, spectroscopic experiments revealed large differences in the environment around Gln41 in Ca·ATP·, Mg·ATP·, and Mg·ADP·G-actin (*12*).

In subdomain 2, there is a loop region, which can be cleaved by chymotrypsin (*13*), subtilisin (*14, 15*), and other proteases (*16*). Subtilisin cleaves the loop selectively at two sites (Met47-Gly48 and Gly42-Val43). The resulting core fragment of 36 kDa and small peptides remain associated with one another under nondenaturing conditions. The cleaved actin possesses the original functions of actin, *e.g.* salt-induced polymerization, activation of myosin ATPase, and DNaseI binding (*14*). Therefore, subtilisin-cleaved actin has been used as a tool to study functional regions of actin (*15, 17*).

In this work, we examined that the influence of structural perturbation of subdomain 2 on the nucleotide and divalent cation-binding mechanism of G-actin. The affinities of both tightly-bound Ca^{2+} and ATP for G-actin were weakened by subtilisin cleavage. The association rate constant of Ca^{2+} to G-actin was reduced by an order of magnitude. We also discuss the stabilization by Ca^{2+} of bound ATP on cleaved G-actin.

MATERIALS AND METHODS

Chemicals—ATP and ADP were obtained from Boehringer Mannheim, εATP from Molecular Probes, Quin 2 from Dojindo Laboratories, and subtilisin Carlsberg from Sigma. All other materials were of reagent grade.

Proteins—G-Actin of rabbit skeletal muscle was prepared from acetone-dried powder according to Suzuki and Mihashi (*18*) and stored in G-buffer (pH 8.0) consisting of 1 mM Tris-HCl, 0.2 mM $CaCl_2$, 0.2 mM ATP, 1 mM NaN_3, and 1 mM 2-mercaptoethanol on ice.

Subtilisin cleavage of G-actin was performed by the method of Schwyter *et al.* (*14*) with a slight modification as

[1] To whom correspondence should be addressed. Phone: +81-592-31-9563, Fax: +81-592-31-9557, e-mail: ooi@bio.mie-u.ac.jp

Abbreviations: εATP, 1,N^6-ethenoadenosine 5′-triphosphate; DNaseI, deoxyribonuclease I; Quin 2, 8-amino-2-[(2-amino-5-methylphenoxy)methyl]-6-methoxyquinoline-*N,N,N′,N′*-tetraacetic acid; metal-free, divalent cation-free.

follows. G-Actin (2–3 mg/ml) was digested with subtilisin at a ratio of 1 : 1,000 (w/w) for 30 min at 20°C. The reaction was stopped by the addition of 1 mM phenylmethanesulfonyl fluoride. The cleaved G-actin was polymerized in 2 mM $MgCl_2$, 60 mM KCl, 1 mM ATP, 10 mM HEPES (pH 7.5) for 1 h at 20°C. After centrifugation, the pellet was homogenized in the same buffer by a brief sonication and then resedimented. The pellet was suspended in and dialyzed against G-buffer, in which the concentrations of both ATP and $CaCl_2$ were increased to 0.4 mM. The degree of digestion was checked with a chromato-scanner (Shimadzu CS-910) on Coomassie Brilliant Blue-stained SDS-PAGE gel. All experiments on cleaved G-actin were done with the product whose purity was greater than 99.5%. The purified cleaved G-actin was used within 2 days after cleavage. Subtilisin-cleaved G-actin loses the ability to undergo salt-induced polymerization after removal of the pentapeptide Val43-Met47 (*15*). Since we purified the cleaved G-actin by means of a polymerization-depolymerization cycle, the prepared cleaved G-actin consisted of only the polymerizable form. Inactivation of the cleaved G-actin during the storage on ice was checked by testing its polymerization. Up to at least 3 days of storage, we found no difference in the critical concentration, which was 0.5 μM under the conditions of 1 mM $MgCl_2$, 20 mM KCl, and pH 7.0 at 25°C.

To obtain G-actin bound to εATP, polymerized actin was centrifuged, then suspended in G-buffer containing 0.2 mM εATP in place of ATP, and dialyzed against the same buffer.

G-Actin concentration was determined from the absorbance at 290 nm using an extinction coefficient of 0.63 $cm^2 \cdot mg^{-1}$ and a molecular mass of 42 kDa. Protein concentrations of subtilisin-cleaved G-actin and G-actin bound to εATP were determined by means of the Bradford assay using unmodified G-actin as the standard.

Fluorescence Measurements—Fluorescence measurements were made in a Hitachi F-4010 fluorescence spectrophotometer equipped with a thermobath set at 25 ± 0.5°C. The excitation and emission wavelengths were as follows: εATP, excitation at 365 nm and emission at 410 nm; Quin2, excitation at 339 nm and emission at 492 nm; the intrinsic fluorescence of actin, excitation at 297 nm and emission at 329 nm.

Kinetic Analysis of Nucleotide Binding to G-Actin—The nucleotide binding kinetics of cleaved G-actin was analyzed in terms of Scheme 1, which was proposed to describe the equilibrium binding of the ternary complex of G-actin, nucleotide, and divalent cation (*2, 4, 5*); where A stands for G-actin, M for divalent cation, and N for nucleotide. In this scheme, the nucleotide dissociates from G-actin *via* two paths. One is dissociation from metal-free actin (k_{24}), which follows the rate-limiting divalent cation release (k_{12}). This route is referred to as the sequential dissociation route in this paper. In the other route, which is referred to as the complex dissociation route, nucleotide dissociates from the ternary complex as a metal-nucleotide complex (k_{13}).

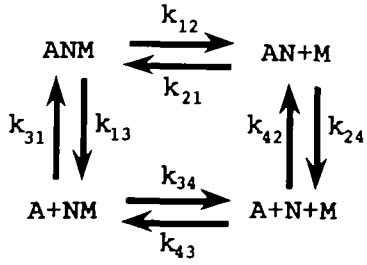

Scheme 1

In Scheme 1, the apparent rate of ATP dissociation (k_{-ATP}) varies with free Ca^{2+} concentration according to the following equation (*4*).

$$k_{-ATP} = \frac{k_{12}}{1 + \frac{k_{21}[M]}{k_{24}}} + k_{13} \quad (1)$$

The first term of this equation represents the sequential dissociation of ATP and the second term represents the complex dissociation. The above equation shows that k_{-ATP} decreases inversely with respect to free Ca^{2+} concentration. When $[M] \gg k_{24}/k_{21}$, the rate is not expected to vary with Ca^{2+} concentration ($k_{-ATP} \cong k_{13}$).

Dissociation Rate of ATP from G-Actin—k_{-ATP} was determined by exchanging bound ATP with a large excess of εATP. In a typical experiment, G-actin solution was diluted into a buffer (pH 7.5) containing the desired amount of Ca^{2+}, 2 mM Tris-HCl, and 2 mM 2-mercaptoethanol to a final concentration of 0.5 μM. Immediately, the reaction was started by the addition of 200 μM εATP. The time course of fluorescence intensity was recorded and then fitted with a single exponential function. Calculation of free Ca^{2+} concentration was accomplished using the literature value of 12 μM for the dissociation constant of Ca·ATP (*19*). The free ATP concentration derived from G-actin solution was in the range of 1–2 μM, so that the reassociation of ATP with G-actin could be neglected. The excitation wavelength of 365 nm was selected. The absorbance of the solution at 365 nm was smaller than 0.01, so that the inner filter effect could be neglected.

Affinity of Ca^{2+} for G-Actin—The affinity of tightly bound Ca^{2+} for G-actin was determined from the equilibrium binding of Ca^{2+} to G-actin as described by Gershman *et al.* (*20*) with a slight modification. The Ca^{2+} release induced by Quin 2 was measured in the presence of 600 μM ATP at pH 7.5. Free Ca^{2+} concentration was calculated using a literature value of 38 nM for the dissociation constant of Ca·Quin 2 (*21, 22*).

Affinity of ATP for Metal-Free Actin—We determined the affinity of ATP for metal-free G-actin by the following method. When the tightly bound nucleotide is removed, G-actin denatures irreversibly (*23*). The denaturation process can be diagrammed as follows:

$$AN \overset{K_N}{\rightleftharpoons} A + N \overset{k_{denat}}{\longrightarrow} \text{denatured A} \qquad \text{Scheme 2}$$

where k_{denat} is the denaturation rate constant, and K_N is the equilibrium dissociation constant of ATP from metal-free G-actin. With a rapid equilibrium assumption between ATP and metal-free actin, the apparent denaturation rate (k_{exp}) is expressed by $k_{denat}/(1 + [ATP]/K_N)$ (*4, 24*). Therefore, one can determine K_N from the dependence of k_{exp} on ATP concentration.

We obtained k_{exp} using the intrinsic fluorescence of actin, as described (*4, 25*). Briefly, after removal of the bound Ca^{2+} with 1 mM EDTA on ice, G-actin solution was immediately diluted into a buffer (pH 7.5) containing 2 mM Tris-HCl, 2 mM 2-mercaptoethanol, and the desired amount of

ATP. The fluorescence decrease was recorded as a measure of denaturation.

Relative Binding Constants of G-Actin for ATP, εATP, and ADP—Relative binding constants, which were defined as the ratio of the equilibrium binding constants of G-actin for ATP, εATP, and ADP, were determined by means of fluorescence titration experiments according to the method of Waechter and Engel (*3*).

RESULTS

Dependence of the Apparent Dissociation Rate of ATP on Free Ca^{2+} Concentration from Intact and Cleaved G-Actin—The kinetics of ATP binding to G-actin was investigated in terms of Scheme 1. The fluorescence of εATP is known to increase upon binding to G-actin (*26*). By taking advantage of this fluorescence property of εATP, the time course of the exchange of actin-bound ATP with free εATP could be measured in the presence of a large excess of εATP. In Fig. 1, the obtained apparent rates (k_{-ATP}) were plotted as a function of free Ca^{2+} concentration. As expected from Eq. 1, k_{-ATP} of cleaved G-actin sharply decreased with increasing free Ca^{2+} and reached a minimum at high Ca^{2+} concentrations. The similarity of the Ca^{2+} dependence of k_{-ATP} between intact and cleaved G-actin indicated that the regulation by Ca^{2+} of nucleotide binding to G-actin remained after subtilisin treatment. In other words, Scheme 1 is applicable to cleaved G-actin.

The results in Fig. 1 showed that k_{-ATP} of cleaved G-actin was larger than that of intact G-actin over the whole range of Ca^{2+}. Subtilisin treatment accelerated the dissociation of bound ATP from G-actin. The apparent rate at the Ca^{2+}-saturated level in Fig. 1 corresponds to k_{13} in Eq. 1. The values of k_{13} thus obtained were 0.0003 and 0.00085 s^{-1} for intact and cleaved G-actin, respectively. The complex dissociation was 2.8-fold faster than that of intact G-actin, suggesting that the stabilization by Ca^{2+} of ATP became weak in cleaved G-actin.

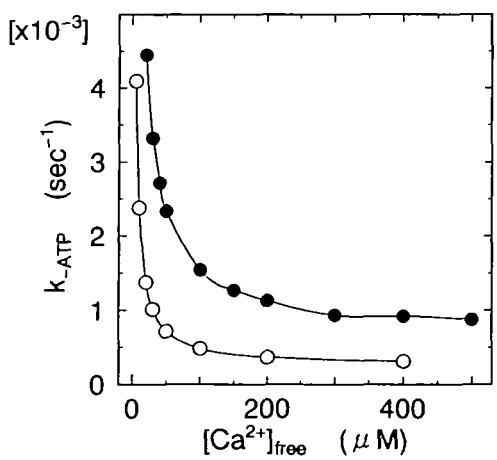

Fig. 1. **Dependence of the apparent dissociation rate of ATP on free Ca^{2+} concentration.** The apparent dissociation rates are plotted *versus* free Ca^{2+} concentration. Open circles represent data for intact G-actin. Closed circles represent those for cleaved G-actin. The k_{13} values were determined by extrapolation to be 0.0003 and 0.00085 s^{-1} for intact G-actin and cleaved G-actin, respectively. Conditions: 0.5 μM intact or cleaved G-actin, 2 mM Tris-HCl, 2 mM 2-mercaptoethanol, 200 μM εATP, pH 7.5, and 25°C.

According to Scheme 1, if the sequential dissociation of ATP is influenced by subtilisin cleavage, the effect appears in the low Ca^{2+} range. As can be seen in Fig. 1, the Ca^{2+} dependence of k_{-ATP} at low Ca^{2+} concentrations was weak in cleaved G-actin. To make this effect clear, we measured k_{-ATP} at concentrations of free Ca^{2+} below 8 μM.

To obtain the apparent rates of the sequential dissociation, we subtracted the experimentally obtained k_{13} from k_{-ATP}. Then the reciprocal of ($k_{-ATP} - k_{13}$) was plotted *versus* free Ca^{2+} in Fig. 2. The reciprocal of the intercept on the ordinate of this figure represents k_{12}. The linear least-squares fit yielded values of 0.020 and 0.026 s^{-1} for intact and cleaved G-actin, respectively. Subtilisin treatment did not significantly affect the dissociation rate constant of tightly bound Ca^{2+}, which was in good agreement with previous observations reported by Kasprzak (*17*). The intercept on the abscissa of Fig. 2 represents k_{24}/k_{21}. This ratio for cleaved G-actin was 3.8 μM, which was about three times larger than that of intact G-actin (1.3 μM).

The above results can be summarized as follows. Both the sequential and the complex dissociation routes are affected by subtilisin cleavage. The influence on the sequential dissociation is weak in terms of the dissociation rate constant of tightly bound Ca^{2+}, but significant in terms of the association rate constant of Ca^{2+} (k_{21}) and/or k_{24}.

Affinity of Ca^{2+} for G-Actin—For further investigation of the sequential dissociation of ATP from cleaved G-actin, binding of Ca^{2+} to cleaved G-actin was studied. We measured the equilibrium dissociation constant of Ca^{2+} from cleaved G-actin. In Fig. 3, the time course of Ca^{2+} release in a typical experiment is shown. When Quin 2 was added to G-actin solution (5 μM), a part of the tightly bound Ca^{2+} was released from G-actin. It is clear that the Ca^{2+} release induced by Quin 2 was large in cleaved G-actin. This result showed that the affinity of tightly bound Ca^{2+} for G-actin was significantly decreased by subtilisin cleavage. After the Ca^{2+} release had reached a plateau, excess Mg^{2+} was added to replace residual bound Ca^{2+} (arrows in Fig. 3). The final Ca^{2+} level of cleaved G-actin was almost the same as that of intact G-actin. The total amount of the released

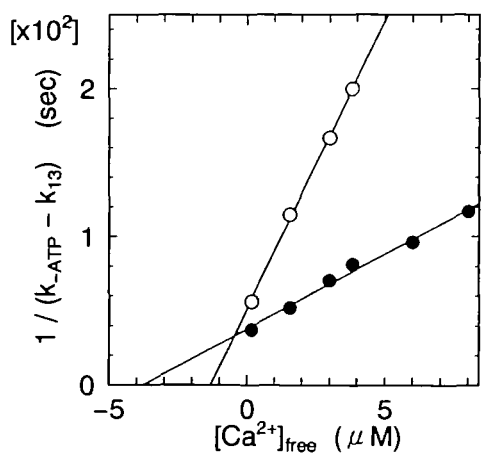

Fig. 2. **Dependence of the rate of the sequential dissociation of ATP on free Ca^{2+} concentration.** The reciprocals of ($k_{-ATP} - k_{13}$) are plotted *versus* free Ca^{2+} concentration (open circles, intact G-actin; closed circles, cleaved G-actin). Solid lines show the results of linear least-squares analysis. Conditions are the same as in the legend to Fig. 1.

Ca^{2+} was about 5 μM in each experiment. It should be noted that the ATP concentration used in these experiments was increased to 600 μM, compared with 200 μM in the original method (*20*). In the experiment on cleaved G-actin, we observed an additional slow increase of Quin 2 fluorescence at lower concentrations of ATP, and this slow phase diminished with increasing concentration of ATP in the solution (results not shown).

To determine K_d of tightly bound Ca^{2+}, we measured bound Ca^{2+} in the presence of various amounts of Quin 2 (Fig. 4). We carried out linear least-squares analysis assuming the binding molar ratio of Ca^{2+} to G-actin to be 1 : 1. Because 1 mol of Ca^{2+} per 1 mol actin was released as mentioned above, this assumption seems appropriate. The obtained values of K_d were 2.9 and 38 nM for intact and cleaved G-actin, respectively. Subtilisin cleavage caused a large decrease in the affinity of bound Ca^{2+}.

In Scheme 1, tightly bound Ca^{2+} is released from G-actin *via* two pathways. As shown in Figs. 1 and 2, the Ca^{2+} release in the complex dissociation route (k_{13}) was 2 orders of magnitude slower than that by sequential dissociation (k_{12}). Therefore, it is reasonable to consider that the determined K_d is equivalent to k_{12}/k_{21}. Since the cleavage had little influence on k_{12}, the low affinity of Ca^{2+} for cleaved G-actin resulted from the greatly decreased k_{21}. The values of k_{21} were calculated to be 6.9×10^6 and 6.8×10^5 $M^{-1}\cdot s^{-1}$ for intact and cleaved G-actin, respectively. Then, from the resulting k_{21} and k_{24}/k_{21} (results in Fig. 2), the k_{24} values were calculated to be 9.0 and 2.6 s^{-1} for intact and cleaved G-actin, respectively.

As shown in the previous section, the influence of cleavage on the sequential dissociation of ATP was mainly seen in k_{24}/k_{21}. We found that both k_{24} and k_{21} were decreased by subtilisin cleavage. Therefore, the rapid ATP dissociation shown in Fig. 2 did not result from a large dissociation rate constant of ATP, but from the extremely reduced association rate constant of Ca^{2+} to cleaved G-actin.

Affinity of ATP for Metal-Free Actin—We determined K_N, the equilibrium dissociation constant of ATP from metal-free G-actin, by measuring the denaturation rate of metal-free G-actin. The previously reported values of K_N are scattered over a wide range (*4, 19, 24*). Kinosian *et al.* noted that their large distribution was due to the ionic strength effect of high concentrations of ATP, that stabilized nucleotide- and metal-free G-actin (*4*). Therefore, we measured the apparent denaturation rate (k_{exp}) in the low ATP concentration range (up to 60 μM). The reciprocals of k_{exp} are plotted as a function of ATP concentration in Fig. 5. Linear regression for intact G-actin yielded values of 0.09 s^{-1} and 3.7 μM for k_{denat} and K_N, respectively, which are in agreement with previously reported values using the same procedure (*4*). In the whole range of ATP concentration, cleaved G-actin denatured more rapidly. The values of k_{denat} and K_N were 0.25 s^{-1} and 6.1 μM, respectively. Subtilisin cleavage reduced the affinity of ATP for metal-free G-actin by a factor of 0.6.

K_N is represented by k_{24}/k_{+2}, using the kinetic constants of Scheme 1. Because the equilibrium between nucleotide and metal-free intact G-actin was rapid compared with the denaturation rate, our rapid equilibrium assumption provides a fairly good approximation for intact G-actin. On the other hand, because of the slow equilibrium between ATP and metal-free G-actin ($k_{24}=2.6$ s^{-1}) and the large denaturation rate constant ($k_{denat}=0.25$ s^{-1}), the obtained value of K_N for cleaved G-actin needed correction. We estimated the systematic error in the case of K_N of cleaved G-actin as follows. Strzelecka-Golaszewska *et al.* derived an equation for k_{exp} with a steady-state assumption (*27*). In their equation, the slope and the intercept on the ordinate of the reciprocal plot are $1/(K_N\cdot k_{denat})$ and $1/k_{denat}+1/k_{24}$, re-

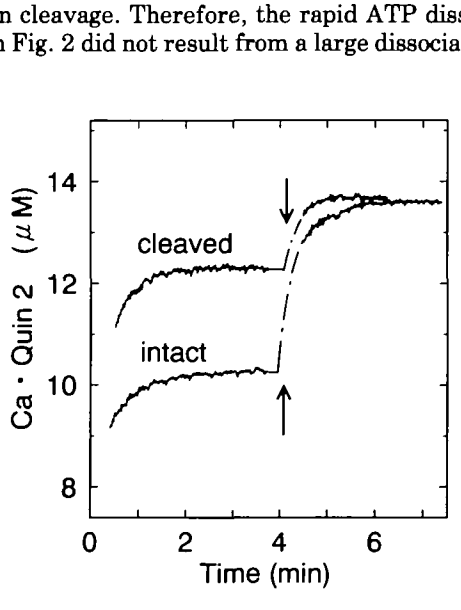

Fig. 3. **Time course of Ca^{2+} dissociation induced by Quin 2.** Time course of Ca^{2+} dissociation was monitored in terms of the fluorescence of Quin 2. At time = 0, Quin 2 was added to 5 μM G-actin solution. After the release of Ca^{2+} had reached a plateau, the remaining bound Ca^{2+} was replaced by the addition of 100 μM Mg^{2+} (indicated by the arrow). The ordinate represents Ca•Quin 2 concentration, which was converted from the fluorescence intensity of Quin 2 by using a calibration curve. The amount of Ca^{2+} derived from G-buffer was 8.5 μM. Conditions: 5 μM G-actin, 5 mM Tris-HCl, 2 mM 2-mercaptoethanol, 600 μM ATP, 50 μM Quin 2, pH 7.5, and 25°C.

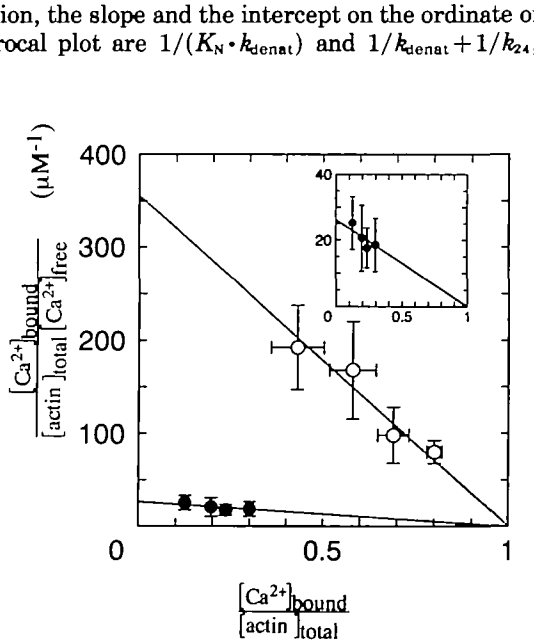

Fig. 4. **Scatchard plots of equilibrium binding of Ca^{2+}.** Scatchard plots of equilibrium binding to intact G-actin (open circles) or to cleaved G-actin (closed circles) are shown. Error bars indicate standard deviation for 3-4 experiments. Solid lines show the results of linear least-squares analysis with the assumption of 1:1 binding (see "RESULTS"). Conditions: 5 μM G-actin, 5 mM Tris-HCl, 2 mM 2-mercaptoethanol, 600 μM ATP, pH 7.5, and 25°C. The inset shows the same data for cleaved G-actin with another scale of the ordinate.

spectively. As the intercept on the ordinate of Fig. 5 was 1/0.25 and the k_{24} value was 2.6, the obtained k_{denat} was underestimated to the extent of about 10%. Therefore, the obtained K_N suffered from an error of about 10%.

Summary of Kinetic and Equilibrium Constants of ATP Binding to Cleaved G-Actin—The kinetic and equilibrium constants for the nucleotide and Ca^{2+} binding of subtilisin cleaved G-actin are summarized in Table I. It can be seen that the ATP binding of G-actin was greatly influenced by subtilisin treatment. The association rate constant of Ca^{2+} to ATP·G-actin was decreased by about 10-fold. Consequently, the affinity of Ca^{2+} for cleaved G-actin was weakened by one order of magnitude. The dissociation rate constant of ATP in the complex dissociation route was 2.8-fold larger than that of intact G-actin. In contrast, the dissociation rate constant of ATP from metal-free G-actin was decreased by 3.5-fold due to subtilisin cleavage. The apparent rapid dissociation of ATP shown in Fig. 1 was mainly due to the weak interaction of Ca^{2+} with cleaved G-actin. It is noteworthy that both k_{24} and k_{42} of cleaved G-actin were smaller than that of intact G-actin. The equilibrium between ATP and metal-free G-actin slowed down after subtilisin treatment.

Taking into account the thermodynamic relation, $K_3 \cdot K_4 = K_1 \cdot K_2$ (where $K_1 = k_{12}/k_{21}$, $K_2 = k_{24}/k_{42}$, $K_3 = k_{13}/k_{31}$, and $K_4 = k_{34}/k_{43}$) in Scheme 1, we can estimate both K_3 and k_{13}. The literature value of K_4 is 1.2×10^{-5} M (*19*), which was determined under similar conditions. The calculated values of K_3 were 8.9×10^{-10} and 1.9×10^{-8} M for intact and cleaved G-actin, respectively. Using the resulting K_3 and the k_{13} (in Table I), we estimated k_{31} of intact and cleaved G-actin to be 3.4×10^5 and 4.5×10^4 $M^{-1}\cdot s^{-1}$, respectively. The association rate constant of Ca·ATP to G-actin was decreased by about 8-fold after subtilisin treatment.

Relative Binding Affinity of ATP, εATP, ADP for Actin—As shown above, the affinities of both Ca^{2+} and nucleotide for G-actin were weakened by subtilisin cleavage. These results suggested that subtilisin treatment loosened the nucleotide binding region. Therefore, it is important to know whether the ability to distinguish bound nucleotide is altered in cleaved G-actin. We determined the relative affinity for ATP and ADP by the method of Waechter and Engel (*3*). Figure 6 showed the results of the competitive binding of εATP with ATP or ADP. The relative binding constants denoted in the legend to Fig. 6 were determined by the non-linear least-squares method (*28*). The values of K_{ATP}/K_{ADP} were calculated to be 313 and 233 for intact and cleaved G-actin, respectively.

Although the absolute affinity of Ca·ATP (K_3) was

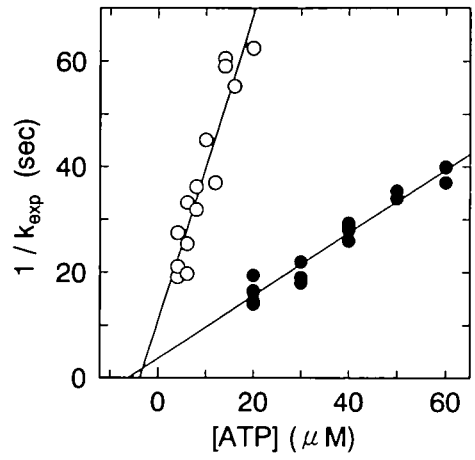

Fig. 5. **Dependence of the denaturation rate on ATP concentration.** The apparent rate of the denaturation (k_{exp}) induced by the removal of tightly bound Ca^{2+} was measured at various concentrations of ATP. The reciprocals of k_{exp} are plotted *versus* ATP concentration (open circles, intact actin; closed circles, cleaved actin). Conditions: 2 μM actin, 2 mM Tris-HCl, 2 mM 2-mercaptoethanol, 1 mM EDTA, pH 7.5, and 25°C.

TABLE I. **Influence of subtilisin cleavage of G-actin on kinetic and equilibrium constants of ATP binding.** Kinetic and equilibrium constants of Scheme 1 are listed. The values of k_{13} and k_{21} were obtained from the nucleotide exchange experiments (Figs. 1 and 2). Equilibrium dissociation constants, k_{12}/k_{21} and k_{24}/k_{42}, were determined in Fig. 4 and Fig. 5, respectively. Other rate constants were calculated from the above constants and k_{24}/k_{21} determined in Fig. 2. Conditions: pH 7.5, 25°C.

	k_{13} (s^{-1})	k_{12} (s^{-1})	k_{21} ($M^{-1}\cdot s^{-1}$)	k_{24} (s^{-1})	k_{42} ($M^{-1}\cdot s^{-1}$)	k_{12}/k_{31} (M)	k_{24}/k_{42} (M)
Intact	0.00030	0.020	6.9×10^6	9.0	2.4×10^6	2.9×10^{-9}	3.7×10^{-6}
Cleaved	0.00085	0.026	6.8×10^5	2.6	4.3×10^5	3.8×10^{-8}	6.1×10^{-6}

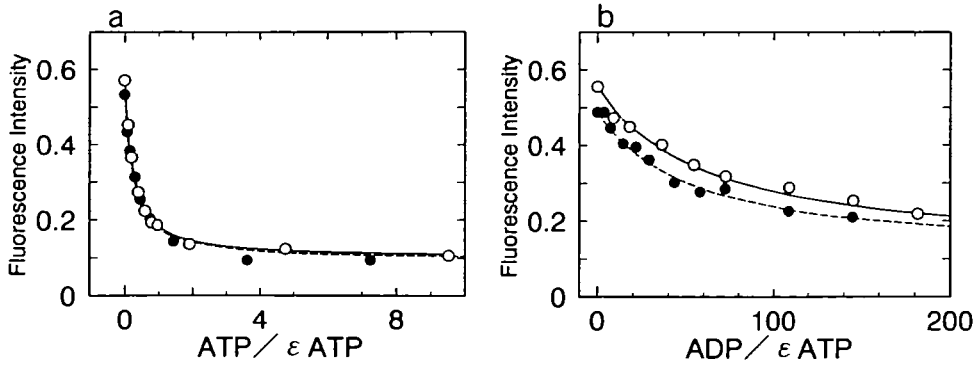

Fig. 6. **Relative binding constants of ATP, εATP, and ADP.** The fluorescence intensity of εATP·G-actin complex is plotted *versus* nucleotide concentration ratio. (a) Titrations of intact and cleaved εATP·G-actin by ATP. Theoretical curves were calculated with $K_{ATP}/K_{\varepsilon ATP} = 4.7$ (solid line) and $K_{ATP}/K_{\varepsilon ATP} = 4.2$ (dashed line) for intact G-actin and cleaved G-actin, respectively. (b) Titrations of intact and cleaved εATP·G-actin by ADP; $K_{ADP}/K_{\varepsilon ATP} = 0.015$ for intact G-actin (solid line), $K_{ADP}/K_{\varepsilon ATP} = 0.018$ for cleaved G-actin (dashed line). Conditions: 0.5 μM G-actin, 2 mM Tris-HCl, 2 mM 2-mercaptoethanol, 200 μM free Ca^{2+}, pH 7.5 at 25°C.

decreased by about 21-fold as shown above, the relative affinities of ATP, εATP, and ADP were not significantly affected by subtilisin cleavage. There is a possibility that the region which recognizes the adenine ring and the phosphates of the nucleotide or Ca•nucleotide complex is conserved after subtilisin treatment.

DISCUSSION

Subtilisin-cleaved G-actin retains most of the original functions of intact G-actin (*14*). In the present study, we showed that the nucleotide binding mechanism of cleaved G-actin is analogous to that of intact G-actin, which is well explained by Scheme 1. The free Ca^{2+} dependence of the ATP dissociation rate of cleaved G-actin is similar to that of intact G-actin. The remarkable influence of the cleavage was observed in the affinity of Ca^{2+} for G-actin. The K_d of tightly bound Ca^{2+} for cleaved G-actin was about 13-fold larger than that for intact G-actin. The large K_d indicates that the equilibrium of the ternary complex is slightly shifted towards dissociation. In Fig. 7, the calculated equilibrium concentrations are illustrated as a function of total Ca^{2+} under the conditions of 100 μM ATP and 50 μM G-actin. At 100 μM Ca^{2+}, the concentrations of metal- and nucleotide-free cleaved G-actin and ATP•cleaved G-actin complex are respectively 0.031 and 0.1 μM, which are one order of magnitude larger than those of intact G-actin. In addition to the large k_{denat} (Fig. 4), these results indicate that cleaved G-actin is less stable than intact G-actin under usual experimental conditions.

Tightly bound cation plays a role in linking the nucleotide to the cleft of G-actin. The low affinity of Ca^{2+} for cleaved G-actin results in weak stabilization of bound ATP by Ca^{2+}. In our study, the affinity of ATP for intact G-actin was strengthened 4,200-fold upon binding of Ca^{2+} to actin (K_2/K_3). On the other hand, K_2/K_3 of cleaved G-actin was only 320. In cleaved G-actin, the regulation by Ca^{2+} of ATP affinity was one order of magnitude lower. The "switch mechanism" proposed by Kinosian *et al.* (*4*) was abrogated by subtilisin treatment.

In order to cast light on the dynamic aspects of the weak regulation in cleaved G-actin, the effects of Ca^{2+} on the kinetic rate constants are summarized in Table II. To represent the magnitude of the influence of Ca^{2+}, we defined the λ value, which is the ratio of the kinetic rate constant in the absence of Ca^{2+} to that in the presence of Ca^{2+}. For both intact and cleaved G-actins, the λ^{off} value was extremely large compared with λ^{on}. The Ca^{2+}-regulation of ATP affinity was performed mostly by decreasing the dissociation rate constant of ATP. This suggests that Ca^{2+} suppresses the relative motion between the small and large domains and/or the fluctuation of the nucleotide binding site. Although the association rate constants in the presence and in the absence of Ca^{2+} were both greatly decreased by subtilisin cleavage, the λ^{on} value of cleaved G-actin was essentially unchanged from that of intact G-actin. On the other hand, λ^{off} was about 10-fold smaller than that of intact G-actin. Thus, the desensitization in Ca^{2+}-regulation of ATP affinity was a consequence of incomplete suppression of the dissociation rate constant of ATP. There are two factors in the incomplete suppression. One is the large dissociation rate constant of Ca•ATP due to the weak interaction between cleaved G-actin and Ca^{2+}. The other is the small dissociation rate constant of ATP in the absence of tightly bound Ca^{2+}, which makes the suppression by Ca^{2+} less effective.

The high hydrophobicity of the loop suggests that it is not in a stable position or in a definite configuration. McLaughlin *et al.* concluded that the loop region is mobile or disordered from a comparison between atomic models of actin-gelsolin segment 1 and actin-DNaseI complex (*29*). It is reasonable to consider that the loop can not stay in its original position after subtilisin cleavage. Under thermal equilibrium condition, the cleaved loop will take up a more

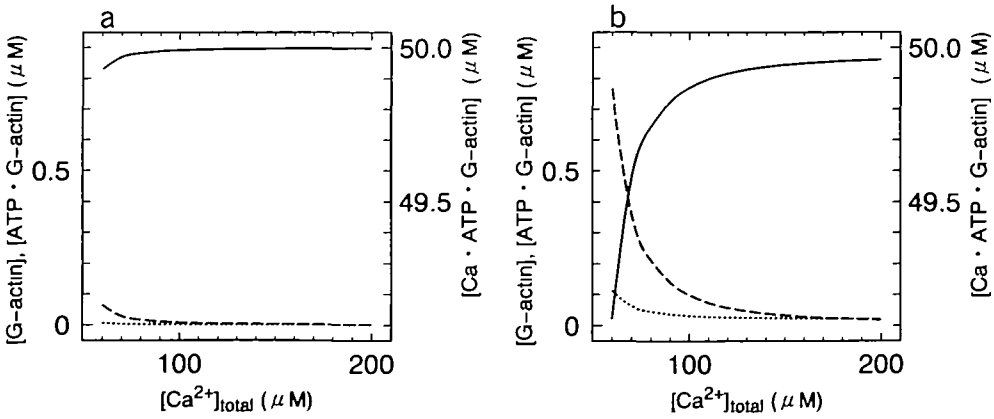

Fig. 7. **Calculation of the equilibrium concentrations.** The concentrations of G-actin species present at equilibrium were calculated at the desired amount of Ca^{2+}. Concentrations of Ca•ATP•G-actin (solid line), ATP•G-actin (dashed line), and metal- and nucleotide-free G-actin (dotted line) are plotted as a function of total Ca^{2+} concentration. (a) intact G-actin. (b) cleaved G-actin. The concentration of Ca•ATP•G-actin is represented on the right-hand axis. Conditions: 50 μM total actin, 100 μM total ATP.

TABLE II. **Effects of Ca^{2+} on the rate constants of ATP binding.** The values of k_{24}, k_{42}, k_{13}, and k_{31} are listed. That of k_{31} was calculated from k_{13} and k_{13}/k_{31} using thermodynamic consistency (see "RESULTS"). The λ value was defined as the ratio of the rate constant in the absence of Ca^{2+} to that in the presence of Ca^{2+}.

	Association rate constant ($M^{-1}\cdot s^{-1}$)		λ^{on}	Dissociation rate constant (s^{-1})		λ^{off}
	−Ca (k_{42})	+Ca (k_{31})		−Ca (k_{24})	+Ca (k_{13})	
Intact	2.4×10^6	3.4×10^5	7.1	9.0	0.00030	30,000
Cleaved	4.3×10^5	4.5×10^4	9.6	2.6	0.00085	3,100

stable configuration and become less mobile than before subtilisin cleavage. The slow equilibrium between ATP and metal-free G-actin revealed in this work may have resulted from such a conformational rearrangement of the loop and/or subdomain 2.

In conclusion, the affinity of tightly bound Ca^{2+} to G-actin was significantly decreased by subtilisin cleavage. The low affinity of bound Ca^{2+} led to the destabilization of bound ATP on cleaved G-actin. Our results also revealed that subtilisin treatment caused the ATP exchange of metal-free G-actin to become slow.

REFERENCES

1. Oosawa, F. and Kasai, M. (1971) Actin in *Subunits in Biological Systems* (Timasheff, S.N. and Fasman, G.D., eds.) Vol. 5, part A, pp. 261-322, Dekker, New York
2. Kuehl, W.M. and Gergely, J. (1969) The kinetics of exchange of adenosine triphosphate and calcium with G-actin. *J. Biol. Chem.* **244**, 4720-4729
3. Waechter, F. and Engel, J. (1975) The kinetics of the exchange of G-actin-bound 1:N^6-ethenoadenosine 5′-triphosphate with ATP as followed by fluorescence. *Eur. J. Biochem.* **57**, 453-459
4. Kinosian, H.J., Selden, L.A., Estes, J.E., and Gershman, L.C. (1993) Nucleotide binding to actin: Cation dependence of nucleotide dissociation and exchange rates. *J. Biol. Chem.* **268**, 8683-8691
5. Valentin-Ranc, C. and Carlier, M.-F. (1989) Evidence for the direct interaction between tightly bound divalent metal ion and ATP on actin: Binding of the Λ isomers of $\beta\gamma$-bidentate CrATP to actin. *J. Biol. Chem.* **264**, 20871-20880
6. Kabsch, W., Mannherz, H.G., Suck, D., Pai, E.F., and Holmes, K. C. (1990) Atomic structure of the actin: DNase I complex. *Nature* **347**, 37-44
7. Frieden, C. (1982) The Mg^{2+}-induced conformational change in rabbit skeletal muscle G-actin. *J. Biol. Chem.* **257**, 2882-2886
8. Freiden, C. and Patane, K. (1985) Differences in G-actin containing bound ATP or ADP: The Mg^{2+}-induced conformational change requires ATP. *Biochemistry* **24**, 4192-4196
9. Crosbie, R.H., Miller, C., Cheung, P., Goodnight, T., Muhlrad, A., and Reisler, E. (1994) Structural connectivity in actin: Effect of C-terminal modifications on the properties of actin. *Biophys. J.* **67**, 1957-1964
10. Strzelecka-Golaszewska, H., Mossakowska, M., Wozniak, A., Moraczewska, J., and Nakayama, H. (1995) Long-range conformational effects of proteolytic removal of the last three residues of actin. *Biochem. J.* **307**, 527-534
11. Strzelecka-Golaszewska, H., Moraczewska, J., Khaitlina, S.Y., and Mossakowska, M. (1993) Localization of the tightly bound divalent-cation-dependent and nucleotide-dependent conformation changes in G-actin using limited proteolytic digestion. *Eur. J. Biochem.* **211**, 731-742
12. Kim, E., Motoki, M., Seguro, K., Muhlrad, A., and Reisler, E. (1995) Conformational changes in subdomain 2 of G-actin: Fluorescence probing by dansyl ethylenediamine attached to Gln-41. *Biophys. J.* **69**, 2024-2032
13. Konno, K. (1987) Functional, chymotryptically split actin and its interaction with myosin subfragment 1. *Biochemistry* **26**, 3582-3589
14. Schwyter, D., Phillips, M., and Reisler, E. (1989) Subtilisin-cleaved actin: Polymerization and interaction with myosin subfragment 1. *Biochemistry* **28**, 5889-5895
15. Kiessling, P., Jahn, W., Maier, G., Polzar, B., and Mannherz, H.G. (1995) Purification and characterization of subtilisin cleaved actin lacking the segment of residues 43-47 in the DNase I binding loop. *Biochemistry* **34**, 14834-14842
16. Higashi-Fujime, S., Suzuki, M., Titani, K., and Hozumi, T. (1992) Muscle actin cleaved by proteinase K: Its polymerization and *in vitro* motility. *J. Biochem.* **112**, 568-572
17. Kasprzak, A.A. (1993) Myosin subfragment 1 inhibits dissociation of nucleotide and calcium from G-actin. *J. Biol. Chem.* **268**, 13261-13266
18. Suzuki, N. and Mihashi, M. (1991) Binding mode of cytochalasin B to F-actin is altered by lateral binding of regulatory proteins. *J. Biochem.* **109**, 19-23
19. Nowak, E., Strzelecka-Golaszewska, H., and Goody, R.S. (1988) Kinetics of nucleotide and metal ion interaction with G-actin. *Biochemistry* **27**, 1785-1792
20. Gershman, L.C., Selden, L.A., and Estes, J.E. (1986) High affinity binding of divalent cation to actin monomer is much stronger than previously reported. *Biochem. Biophys. Res. Commun.* **135**, 607-614
21. Gershman, L.C., Selden, L.A., and Estes, J.E. (1991) High affinity divalent cation exchange on actin: Association rate measurements support the simple competitive model. *J. Biol. Chem.* **266**, 76-82
22. Estes, J.E., Selden, L.A., and Gershman, L.C. (1987) Tight binding of divalent cations to monomeric actin: Binding kinetics support a simplified model. *J. Biol. Chem.* **262**, 4952-4957
23. Asakura, S. (1961) The interaction between G-actin and ATP. *Arch. Biochem. Biophys.* **92**, 140-149
24. Valentin-Ranc, C. and Carlier, M.-F. (1991) Role of ATP-bound divalent metal ion in the conformation and function of actin: Comparison of Mg-ATP, Ca-ATP, and metal ion-free ATP-actin. *J. Biol. Chem.* **266**, 7668-7675
25. Lehrer, S.S. and Kerwar, G. (1972) Intrinsic fluorescence of actin. *Biochemistry* **11**, 1211-1217
26. Miki, M., Ohnuma, H., and Mihashi, K. (1974) Interaction of actin water ε-ATP. *FEBS Lett.* **46**, 17-19
27. Strzelecka-Golaszewska, H., Venyaminov, S.Y., Zmorzynski, S., and Mossakowska, M. (1985) Effects of various amino acid replacements on the conformational stability of G-actin. *Eur. J. Biochem.* **147**, 331-342
28. Neidl, C. and Engel, J. (1979) Exchange of ADP, ATP and 1:N^6-ethenoadenosine 5′-triphosphate at G-actin: Equilibrium and kinetics. *Eur. J. Biochem.* **101**, 163-169
29. McLaughlin, P.J., Gooch, J.T., Mannherz, H.-G., and Weeds, A.G. (1993) Structure of gelsolin segment 1-actin complex and the mechanism of filament severing. *Nature* **364**, 685-692